2009

Serendipitous XMM-Newton detection of x-ray emission from the bipolar planetary Nebula Hb 5

Rodolfo Montez

Joel Kastner

Bruce Balick

Accepted by *The Astrophysical Journal*

Serendipitous XMM-Newton Detection of X-ray Emission from the Bipolar Planetary Nebula Hb 5

Rodolfo Montez Jr. and Joel H. Kastner

Chester F. Carlson Center for Imaging Science, Rochester Institute of Technology, Rochester, NY 14623

rodolfo.montez.jr@gmail.com,jhk@cis.rit.edu

Bruce Balick

Department of Astronomy, University of Washington, Seattle, WA 98195-1580

balick@astro.washington.edu

and

Adam Frank

Department of Physics and Astronomy and C. E. K. Mees Observatory, University of Rochester, Rochester, NY 14627-0171

afrank@pas.rochester.edu

ABSTRACT

We report the serendipitous detection by the XMM-Newton X-ray Observatory of an X-ray source at the position of the Type I (He- and N-rich) bipolar planetary nebula Hb 5. The Hb 5 X-ray source appears marginally resolved. While the small number of total counts (~ 170) and significant off-axis angle of the X-ray source ($\sim 7.8'$) precludes a definitive spatial analysis, the morphology of the X-ray emission appears to trace the brightest features seen in optical images of Hb 5. The X-ray spectrum is indicative of a thermal plasma at a temperature between 2.4 and 3.7 MK and appears to display strong Neon emission. The inferred X-ray luminosity is $L_X = 1.5 \times 10^{32}$ ergs s^{-1}. These results suggest that the detected X-ray emission is dominated by shock-heated gas in the bipolar nebula, although we cannot rule out the presence of a point-like component at the position of the central star. The implications for and correspondence with current models of shock-heated gas in planetary nebulae is discussed.

Subject headings: planetary nebulae: individual(PN Hb 5) — X-rays: individual(PN Hb 5)

1. Introduction

The shaping and evolution of planetary nebulae (PNe) has been an active field of study for a few decades and is continually spurred on by new observations that do not fit the existing theoretical models (Balick & Frank 2002, and references therein). Of particular note are the bipolar PNe, with their large lobes and narrow waists, many showing residual evidence of a spherical AGB wind in the form of nested rings centered on the PN central star (Corradi et al. 2004). The implied transition from seemingly spherical mass loss to profoundly bipolar outflow remains an unsolved mystery. Possible shaping and evolutionary mechanisms have been developed ranging from the interacting stellar winds model (Kwok et al. 1978), wherein a hot fast stellar wind shocks a slower moving AGB wind, to collimated flows (Soker 2004; Akashi et al. 2008) possibly launched and shaped by a magnetocentrifugal force fueled by an AGB dynamo (Blackman et al. 2001).

In all of these PN shaping models the presence of gas heated to X-ray emitting temperatures is predicted. The advent of high-spatial-resolution, X-ray observatories (Chandra and XMM-Newton) facilitated the discovery and scrutiny of this shock-heated gas (Guerrero et al. 2005; Kastner et al. 2008, and references therein) and the results were surprising. The observed X-ray temperatures of the shocked plasma have been much lower, $1 - 3 \times 10^6$ K, than predicted, $> 10^7$ K (Stute & Sahai 2006; Kastner et al. 2008), spawning a variety of potential solutions (see Soker & Kastner 2003, for a review). Akashi et al. (2006, 2007, 2008) and Steffen et al. (2008) have since produced more detailed models in an attempt to resolve the temperature discrepancy while adequately reproducing other observed quantities. Steffen et al. (2008) investigate the role played by thermal conduction in establishing the physical properties of the X-ray emitting gas, while Akashi et al. (2006, 2007) consider the possibility that the X-ray emitting gas arose from a slower, post-AGB wind (~ 500 km/s), and Akashi et al. (2008) present numerical simulations that suggest the observed X-ray properties could be explained by jet-wind interaction. These newer models describing PN X-ray emission should, in turn, provide feedback to generalized models describing the origin of the flows shaping PNe, which, taken together, will provide a complete theoretical description of the shaping and evolution of PNe.

The identification of X-ray sources within bipolar PNe should provide unique constraints on this new generation of PN shaping and evolution models. However, thus far such detections have been few and far between (Gruendl et al. 2006; Kastner et al. 2001;

Kastner el al. 2003; Sahai et al. 2003). During an archival program to identify serendipitous X-ray sources associated with PNe, we established that the XMM-Newton Serendipitious Survey[1] includes an X-ray source, 2XMM J174756.2-295937, that is spatially coincident, within errors ($\sim \pm 2''$), with Hubble 5 (Hb 5), a large, narrow-waist bipolar planetary nebula with a bright, compact, core (Pottasch & Surendiranath 2007). Quireza et al. (2007) classify Hb 5 as Peimbert Type I PN, i.e., a He- and N-rich PN descended from a relatively massive progenitor star. Hb 5 is a high-excitation PN and, in particular, is one of the few PNe showing the 7.652 μm Ne VI line (Pottasch & Surendiranath 2007). A photodissociation region immediately surrounding the nebula may account for the presence of molecular hydrogen emission (Bernard-Salas & Tielens 2005; Pottasch & Surendiranath 2007). The distance to Hb 5 is highly uncertain. Rice et al. (2004) derive a distance of 1.4 kpc $\pm$ 0.3 kpc from 3D photoionization modeling, while Pottasch & Surendiranath (2007) argue for a much larger distance, ranging from 3 to 7 kpc. Corradi & Schwarz (1993) find a polar expansion velocity of $\sim$ 250 km s^{-1}, while Pshmish et al. (2000) reported a faster, possibly collimated, wind of 400 km s^{-1} near the center of Hb 5.

2. Analysis

2.1. Data

Hb 5 lies within the field of an XMM-Newton observation of the pulsar PSR J1747-2958 and pulsar wind nebula (MOUSE NEBULA). This observation (ObsID 0152920101) was performed during XMM Revolution 607 on 2003 April 02. The European Photon Imaging Camera (EPIC) detector arrays pn, MOS1, and MOS2 were operated in Full-Frame Mode, with the thick filter, for total exposures of 45.1, 51.3, and 51.3 ks, respectively. We reprocessed the XMM-Newton Observation Data Files using the XMM-Newton Science Analysis Sofware (SAS) package version 7.1.0 with the calibration files available in Current Calibration File Release 241 (XMM-CCF-REL-241). We filtered out high background periods and bad events from all observations using standard filters for imaging mode observations. The resulting net exposure times are 44.1, 50.6, and 50.8 ks, in the pn, MOS1, and MOS2 arrays, respectively.

From the source and background regions used in the spectral extraction of the X-ray source at the position of Hb 5 (described in Section 2.3), we determined that the net source and background count rates in the energy range 0.2-2.0 keV are $1.9 \pm 0.4 \times 10^{-3}$ cnts s^{-1} in

[1]See Watson et al. (2007) for information on the XMM-Newton Serendipitous Survey catalog.

pn, $8.0 \pm 1.8 \times 10^{-4}$ cnts s^{-1} in MOS1, and $8.7 \pm 1.9 \times 10^{-4}$ cnts s^{-1} in MOS2. We merged the three observations using the SAS task *merge*. Using this merged event list, we generated a soft band image for the energy range 0.2-2.0 keV, binned to 5″ pixels (Figure 1a).

2.2. Spatial Analysis

Figure 1a indicates that the X-ray emission at the position of Hb 5 is marginally resolved. Hb 5 is located $\sim 7.8'$ off-axis in the XMM observation, and the coincident X-ray source displays peak emission around 1 keV. This off-axis angle and peak emission are within the range of application of the XMM/EPIC PSF model described in Ghizzardi (2002), i.e., a King profile whose core radius and slope depend on energy and off-axis angle. Specifically, we expect a PSF core radius of 4.71″ and slope of -1.44. This suggests that using a normalized Gaussian smoothing filter with a FWHM of 7.5″ will reduce the loss of information, while aiding our interpretation of the detected X-ray emission. In Figure 1, the smoothed X-ray image contours are overlaid onto the unsmoothed X-ray image (Figure 1a), a 2MASS J-band image (Figure 1b), and a HST WFPC2 F658N ($H\alpha + [NII]$) narrowband image (Figure 1c). The image registration was performed by the IDL Astro Library[2] task *hastrom*. A slight eastward shift ($\sim 0.45''$) of the HST image was required to align the stars appearing in both the 2MASS J-band and chip 3 of the HST WFPC2 F658N fields. Figures 1b and 1c demonstrate that the peak of the X-ray emission coincides with the bright core regions of Hb 5 seen in the 2MASS and HST images, respectively. The apparent extension of the X-ray emission lies along the brightest features observed in the $H\alpha + [NII]$ image.

2.3. Spectral Analysis

The spatial region available for spectral extraction within the XMM image of the Hb 5 field is severely constrained by several unavoidable artifacts. Immediately surrounding the region of interest are chip gaps (in all three EPIC arrays), a bright nearby soft source, and a readout streak from the nearby soft source. Guided by the optical HST position of Hb 5 along with the evident soft X-ray emission, we selected an extraction region that optimized the signal in the spectrum while avoiding these artifacts. An annulus surrounding the source region and omitting nearby sources was used to estimate the background. We used the SAS tasks *rmfgen* and *arfgen* to generate source-specific response matrices and effective area curves; the latter accounts for off-axis vinetting ($\sim 30\%$ loss at $7.8'$, Ehle et al. (2008)).

[2]http://idlastro.gsfc.nasa.gov

The resulting spectra from the three EPIC CCD detector arrays were simultaneously fit in XSPEC (version 12.3.1; Arnaud (1996)) with a variable abundance thermal plasma model, *vmekal* (Mewe et al. 1985, 1986; Kaastra 1992; Liedahl et al. 1995), and intervening absorption, *wabs* (Morrison & McCammon 1983). We used the extinction value $C = 1.60$ at Hβ listed in Pottasch & Surendiranath (2007) to fix the column density at $N_H = 6.0 \times 10^{21} cm^{-2}$ and – noting the apparent presence of a strong spectral feature at ~ 1.0 keV that is likely due to Ne IX and Ne X lines – left as free parameters the gas temperature and the abundance of Ne. We fixed all other abundances at their solar values(Anders & Grevesse 1989). Although fixing the abundance of Ne to its solar value results in a global fit that is acceptable, this fit is poor at the spectral feature near 1.0 keV. There is a modest improvement in the fit when we allow the abundance of Ne to be a free parameter. This latter fit is presented in Figure 2. The temperature is found to lie in the range 2.4-3.7 MK (90% confidence range) and the Ne abundance factor lies in the range 1.8-6.9 (90% confidence range) relative to the solar abundance given by Anders & Grevesse (1989). The best model fit indicates an observed 0.2-2.0 keV flux of 7.9×10^{-15} ergs cm^{-2} s^{-1}, and an unabsorbed flux of 1.2×10^{-13} ergs cm^{-2} s^{-1}. We assume a distance of 3.2 kpc after Pottasch & Surendiranath (2007) and find $L_X = 1.5 \times 10^{32} (D/(3.2 \text{ kpc}))^2$ ergs s^{-1}.

3. Discussion

Hb 5 is the fourth bipolar PNe – after NGC 7026 (Gruendl et al. 2006), the transitional object NGC 7027 (Kastner et al. 2001), and the possibly symbiotic system Mz 3 (Kastner el al. 2003) – with suspected diffuse X-ray emission and only the second Type I PN known to display X-ray emission. The other Type I PN with evidence for shocked X-ray emission is the [WC] PN NGC 5315, which was also discovered serendipitously, far off-axis, by the Chandra X-ray Observatory (Kastner et al. 2008). Indeed, the X-ray emission regions detected in Hb 5 and NGC 5315 display similar characteristics, despite the fact that one is associated with a high excitation, bipolar PN and the other with a compact [WC] PN. Specifically, these two PNe have similar plasma temperatures (within errors) and similar X-ray luminosities (though the L_X values are very uncertain, due to distance uncertainties). In addition, both appear to show strong X-ray Ne lines. Pottasch & Surendiranath (2007) find an Ne abundance factor of 2.2 relative to solar in the infrared spectrum of Hb 5, similar to the (uncertain) overabundance tentatively determined from the X-ray spectrum.

The bipolar PNe detected thus far have closed bipolar lobes, while many of the bipolar PNe observed but not detected have open bipolar lobes (Gruendl et al. 2006). The role of open and closed lobes is an important factor that may determine key characteristics regarding

the presence or absence of hot gas due to wind shocks; open lobes allow the gas to expand and, thus, quickly cool, whereas closed lobes evidently contain the gas, and cooling through heat conduction at the nebular-hot gas boundary may dominate (Steffen et al. 2008). In this regard, it appears significant that the extended X-ray emission in Hb 5 corresponds closely to the brighter regions seen in the HST image, suggesting the X-rays are coming from shocked material within the most tightly confined regions of the lobes.

Recent simulations of axisymmetric jets expanding into a spherical wind by Akashi et al. (2008) reproduced optical features seen in some bipolar PNe. This study focused on Mz 3 and M 1-92, but included simulations with generic PNe parameters. Some of these key optical features are also seen in Hb 5, i.e., an equatorial dense region and bright polar rim. The evidence of a fast, possibly collimated, wind reported by Pshmish et al. (2000) suggests that the extended X-ray emission observed in Hb 5 can likely be traced to a collimated fast wind (Akashi et al. 2006, 2007). The point-symmetric features of the nebula and the extension in the X-ray emission support the possibility of an X-ray jet or shocks from such a collimated flow. The spatial coincidence with the central region of Hb 5 suggests that some X-rays may originate from the core and/or the central star itself. However, caution is warranted, given the small number of counts detected due to vingetting at the large off-axis angle of Hb 5 and the large background due to nearby bright sources convolved with the XMM PSF.

A deep, targeted X-ray observation of Hb 5 might bring our Ne abundance factor into agreement with the infrared-determined value and would decrease the uncertainties in Ne abundance by allowing us to fit the abundances of additional elements. Also, in the archival XMM-Newton observation of Hb 5, small but significant (termination) portions of the bipolar lobes lie in the detector chip gap and the readout streak of the nearby source. Hence, a targeted Chandra X-ray Observatory X-ray observation of Hb 5 would provide the higher spatial resolution imagery that might enhance the role this PN plays in our understanding of the shaping and evolution of planetary nebulae.

4. Conclusions

Our spatial and spectral analysis of a moderately resolved, off-axis, low count XMM-Newton detection of X-ray emission at the location of the bipolar PN Hb 5 leads us to conclude that the emission originates with Hb 5. The X-ray emission is indicative of a thermal plasma at 2.4-3.7 MK with X-ray luminosity of 1.5×10^{32} erg s^{-1}. Comparison with images of infrared and optical emission shows that the peak of the X-ray emission corresponds closely with the bright core of Hb 5 and the extension of the X-ray emission lies along bright extensions in the optical image. The X-ray temperature and luminosity,

as compared to PNe known to exhibit shock-induced X-ray emission (Kastner et al. 2008), further suggest that the emission arises from shocks in the nebula, as opposed to the harder and less luminous X-ray emission associated with central stars (e.g. Mz 3; Kastner el al. (2003)). As only the fourth bipolar PNe with detected X-ray emission, Hb 5 may play an important role in the evolving study of the shaping and evolution of PNe. This PN therefore merits future targeted, deep, high spatial resolution X-ray observation.

This research was supported by NASA Astrophysics Data Analysis Program award NNX08AJ65G to RIT.

Facilities: XMM (EPIC), HST (WFPC2), CTIO:2MASS

REFERENCES

Akashi, M., Soker, N., Behar, E. 2006, MNRAS, 368, 1706

Akashi, M., Soker, N., Behar, E. 2007, MNRAS, 375, 137

Akashi, M., Soker, N., Behar, E. 2008, New Astronomy, 13, 563

Anders, E. & Grevesse, N. 1989, Geochimica and Cosmochimica Acta 53, 197

Arnaud, K.A. 1996, Astronomical Data Analysis Software and Systems V, eds. Jacoby G. and Barnes J., p17, ASP Conf. Series volume 101

Balick, B. & Frank, A. 2002, ARA&A, 40, 439

Bernard-Salas, J. & Tielens, A. G. G. M. 2005, A&A, 431, 523

Blackman, E. G., Frank, A., Markiel, J. A., Thomas, J. H., Van Horn, H. M. 2001, Nature, 409, 485

Chu, Y.-H., Guerrero, M. A., Gruendl, R. A., Williams, R. M., Kaler, J. B. 2001, ApJ, 553, 69

Corradi, R. L. M. & Schwarz, H. E. 1993, A&A, 269, 462

Corradi, R. L. M., Sanchez-Blazquez, P., Mellema, G., Giammanco, C., Schwarz, H. E. 2004, A&A, 417, 637

Ehle, M., de la Calle, I., Daz Trigo, M., Gonzlez Riestra, R., Loiseau, N., Rodrguez, P. 2008, XMM-Newton Users' Handbook, Issue 2.6

Ghizzardi, S. 2002, XMM-Newton Calibration Documentation (XMM-SOC-CAL-TN-0029)

Gruendl, R. A., Guerrero, M. A., Chu, Y.-H., Williams, R. M. 2006, ApJ, 653, 339

Guerrero, M. A., Chu, Y.-H., Gruendl, R. A., Meixner, M. 2005, A&A, 430, L69

Guerrero, M. A., Gruendl, R. A., and Chu, Y.-H. 2002, A&A, 387, L1

Kaastra, J.S. 1992, An X-Ray Spectral Code for Optically Thin Plasmas (Internal SRON-Leiden Report, updated version 2.0)

Kastner, J. H., Montez Jr., R., Balick, B., and De Marco, O. 2008, ApJ, 672, 957

Kastner, J. H., Balick, B., Blackman, E. G., Frank, A., Soker, N., Vrtilek, S. D., Jingqiang, L. 2003, ApJ, 591, 37

Kastner, J. H., Vrtilek, S. D., Soker, N. 2001, ApJ, 550, 189

Kwok, S., Purton, C. R., Fitzgerald, P. M. 1978, ApJ, 219, 125

Liedahl, D.A., Osterheld, A.L., and Goldstein, W.H. 1995, ApJ, 438, 115

Mewe, R., Lemen, J.R., and van den Oord, G.H.J. 1986, A&AS, 65, 511

Mewe, R., Gronenschild, E.H.B.M., and van den Oord, G.H.J. 1985,A&AS, 62, 197

Morrison, R. & McCammon, D. 1983, ApJ, 270, 119

Pishmish, P., Manteiga, M., and Mampaso Recio, A. 2000, Asymmetrical Planetary Nebulae II: From Origins to Microstructures, ASP Conference Series, Edited by J. H. Kastner, N. Soker, and S. Rappaport, 199, 397

Pottasch, S. R. & Surendiranath, R. 2007, A&A, 462, 179

Quireza, C., Rocha-Pinto, H. J., Maciel, W. J., A&A, 475, 217

Rice, M., Schwarz, H., Monteiro, H. 2004, BAAS, 36, 1572

Sahai, R., Kastner, J. H., Frank, A., Morris, M., Blackman, E. G. 2003, ApJ, 599,87

Soker, N. 2004, A&A, 414, 943

Soker, N. & Kastner, J. H. 2003, ApJ, 583, 368

Steffen, M., Schoenberner, D., and Warmuth, A. 2008, *in press*, preprint arXiv:0807.3290

Stute, M. & Sahai, R. 2006, ApJ, 651, 882

Watson et al. (2007), "The XMM-Newton Serendipitous Survey. V. The Second XMM-Newton Serendipitous Source Catalogue,", in preparation.

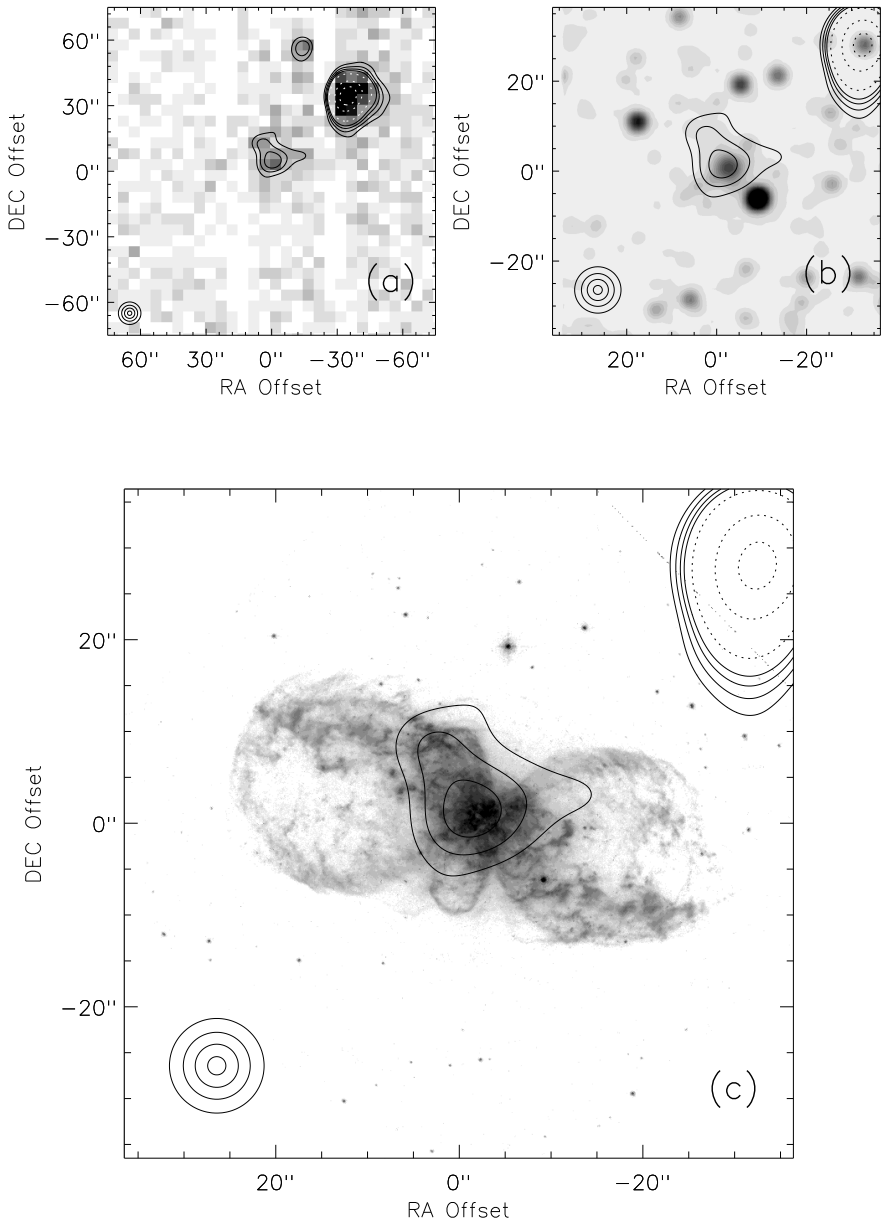

Fig. 1.— XMM imaging of the Hb 5 field. Smoothed X-ray contours at 9, 11, 13, and 15 counts (solid contours) and at 20, 40, and 60 counts (dotted contours) are overlaid upon the (a) unsmoothed XMM X-ray image, (b) 2MASS J-band image, and (c) HST F658N narrowband image ($H\alpha + [NII]$). In the lower left corner of each panel, we display the 25%, 50%, 75% and 90% levels of the normalized Gaussian filter used to smooth the X-ray image.

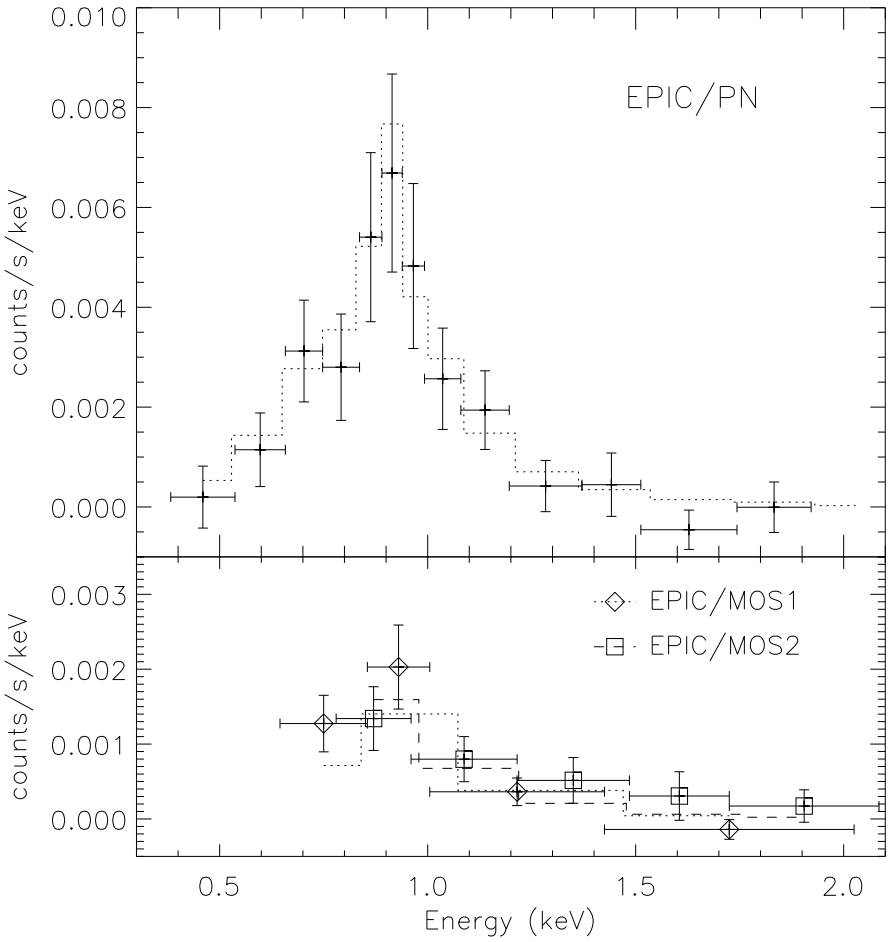

Fig. 2.— X-ray spectra of the Hb 5 source as obtained from the three EPIC CCD detector arrays (crosses, diamonds, and squares; pn: top panel; MOS: bottom panel) overlaid with the result of the best simultaneous fit to a model consisting of a thermal plasma (*vmekal*) and intervening absorption (*wabs*).